GEOLOGICAL SURVEY OF ISRAEL

Ground Movements Detected by PSInSAR:

Haifa and Mt. Carmel, Israel

Ran Novitsky , Gidon Baer

תקציר

בעבודה הנוכחית מוצגות מדידות דפורמציה בסדרת זמן וכן ממוצע שנתי של קצב דפורמציה עבור העיר חיפה והאזור הצפוני של העתק הכרמל, תוך שימוש בשיטת אינטרפרומטריה של מחזירים קבועים (PSInSar).נותחו ארבעים ושבע (47) הדמעות של לוויני **ERS-1** ו- **ERS-2** בין אפריל 1992 לדצמבר 2001. אנו מציגים ניתוח ראשוני וניסיון למצוא התאמה בין הדפורמציות לגורמים שונים כגון: שינויי מפלס מי-תהום (עבור אזור נמל חיפה), פעילות סייסמית, יציבות מדרונות ומודל טקטוני. כרגע, לא נמצאה קורלציה ישירה בין הדפורמציה לפעילות הסיסמית, שינויי מפלס מי-תהום או רגישות לגלישות קרקע. נמצא קורלציה בין תוצאות מדידות הדפורמציה בעזרת אינטרפרומטריה ותצפיות שדה במרכז הקניות "לב המפרץ" בחיפה וכן נעשה ניסיון להסביר את הדפורמציה שנצפתה באזור יוקנעם-צומת ג'למה בעזרת מודל טקטוני המתאר תנועה שמאלית לאורך מקטעי ההעתק שכוונם צפון-מערב.

ABSTRACT

The area of study covers Mt. Carmel between the city of Haifa and Zevulun plane in the north and Menashe Hills in the south. The area is situated adjacent to the Carmel Fault System (CFS), which has been considered to be a potentially active fault (Bartov et al., 2002), and is at a potentially high seismic risk due to the large population and its petrochemical industry and its proximity to the CFS. Although many studies explored the tectonics of the area, little is known about the most recent deformation. This study presents the first results of the current deformation in this area, with spatial resolution higher than ever achieved.

This study was carried out within the framework of the *Terrafirma* Pan-European service for ground motion hazards (for more details see: http://www.terrafirma.eu.com). It presents a preliminary interpretation of PSInSAR measurements made by T.R.E, Milano (http://www.treuropa.com). Measurements of deformation time series and average annual rates were made using the Permanent Scatterers Interferometry (PSInSar) method. Forty seven (47) ERS-1 and ERS-2 scenes between April 1992 and December 2001 were analyzed. An initial interpretation is presented, and an attempt is made to correlate the observed deformation with other features, such as water-level changes, seismicity, slope stability, and tectonic models. For the moment, no clear correlation was found between deformation and seismicity, water-level changes or landslide sensitivity. Some correlation is found between PSInSAR-detected ground movement and field observations in Lev-Hamifratz shopping center. An attempt is also made to explain some of the observed deformation in the Yokne'am – Jalame area by a fault model that assumes left-lateral strike-slip motion along the NW-striking Carmel Fault segments.

Contents

List of Figures

1. Introduction

This study was carried out within the framework of the *Terrafirma* Pan-European service for ground motion hazards (for more details see: http://www.terrafirma.eu.com). It presents a preliminary interpretation of PSInSAR measurements made by T.R.E, Milano (http://www.treuropa.com). Forty seven (47) ERS-1 and ERS-2 scenes between April 1992 and December 2001 were analyzed. The data consist of 35,000 permanent scatterers (PS) of which 16,000 were also analyzed for their time-series behavior. The area of study covers Mt. Carmel between the city of Haifa and Zevulun plane in the north and Menashe Hills in the south. The area is situated adjacent to the Carmel Fault System (CFS), which has been considered to be a potentially active fault (Bartov et al., 2002), and is at a potentially high seismic risk due to the large population and its petrochemical industry and its proximity to the CFS. Although many studies explored the tectonics of the area, little is known about the most recent deformation. This study presents the first results of the current deformation in this area, with spatial resolution higher than ever achieved.

2. Geographical and Geological Context

The city of Haifa is located in northern Israel, on the shores of the Mediterranean Sea and up the slopes of Mt. Carmel (Fig. 1). The city and its surrounding area inhabit more than 700,000 people. Mt. Carmel (~500 m) is an uplifted structure comprising of prominent NNE trending folds that belong to the Late Cretaceous to Tertiary "Syrian Arc" system (Rotstein et al., 1993).

The lithology of Mt. Carmel is composed of dolomite, limestone, chalky limestone, chalk and marl, as well as some volcanic rocks, mainly tuff. To the east of Mt. Carmel is the Zevulun plane which is geologically situated within the Kishon Graben. It is highly populated, and is adjacent to a petrochemical industrial area. The lithology of this area is mainly unconsolidated sediments, consisting of sand, clay and silt overlying sandy-limestone (“Kurkar”), chalk and marl (Kafri and Ecker, 1964).

The Carmel Fault System (CFS) which is one of the major active elements in the eastern Mediterranean, runs along the NE foothills of Mt. Carmel, and is considered to be the largest splay of the Dead-Sea Fault (Rotstein et al., 1993). The CFS divides the crustal structure of northern Israel into two distinct provinces. The part south of the CFS is relatively quiet seismically, whereas the northern part shows a higher rate of seismic activity (Hofstetter et al.,

Fig 1. Location map of the Carmel Fault System (CFS) superimposed on an orhtorectified aerial photograph (orthophoto). The red line marks the main fault described as a potentially active fault (after Bartov et al., 2002. Black lines are surface mapped faults (From GSI GIS database). (1) Yokneam junction. (2) Jalame' junction.

1996, Shamir et al., 2000 ; Fig. 2). Moreover, while the crustal thickness of the southern part is about 30-35 km, the northern part is only 23 km thick (Ginzburg et al. 1994). The CFS is associated with the steep slopes of Mt. Carmel, which form a relief of 350-500 m above the surrounding planes. The fault shows a normal slip component in some places (Achmon, 1998), and horizontal movement, which has been considered by most researchers to be sinistral. De-Sitter (1962) and Freund (1965) estimated a sinistral movement of 10 km based on the offset between anticlinal axes south and north of the CFS. Achmon (1986) and Rotstein (1993) estimated sinistral displacement of about 4000 m. The strike of the CFS changes along its course, from NW east of Menashe Hills to N-S and back to NW in the northwestern segment (Fig. 1). Assuming sinistral movement along the NW-striking fault segments, this geometry should lead to a component of compression on the N-S section (Rotstein et al., 1993), forming a Push-Up structure in the N-S section and Pull-Apart structures along the NW-striking segments (e.g. Kishon graben and Yizre'el valley; Rotstein et al., 2003). Achmon (1986) proposed that the CFS is a wide fault zone rather than a single fault. Rotstein et al. (1993) showed, with high-resolution seismic lines, that the deformation zone near the NW-SE trending segments is about 0.8 km wide while near the N-S trending segment it is about 3 km. The largest earthquake (M=5.3) near the CFS in the last 100 years occurred in August 24, 1984. Paleoseismic research showed that earthquakes with magnitude of 5.5 and greater did not occur along the CFS for the last few tens of thousands of years (Heimann et al., 2001 ; Gluck, 2001).

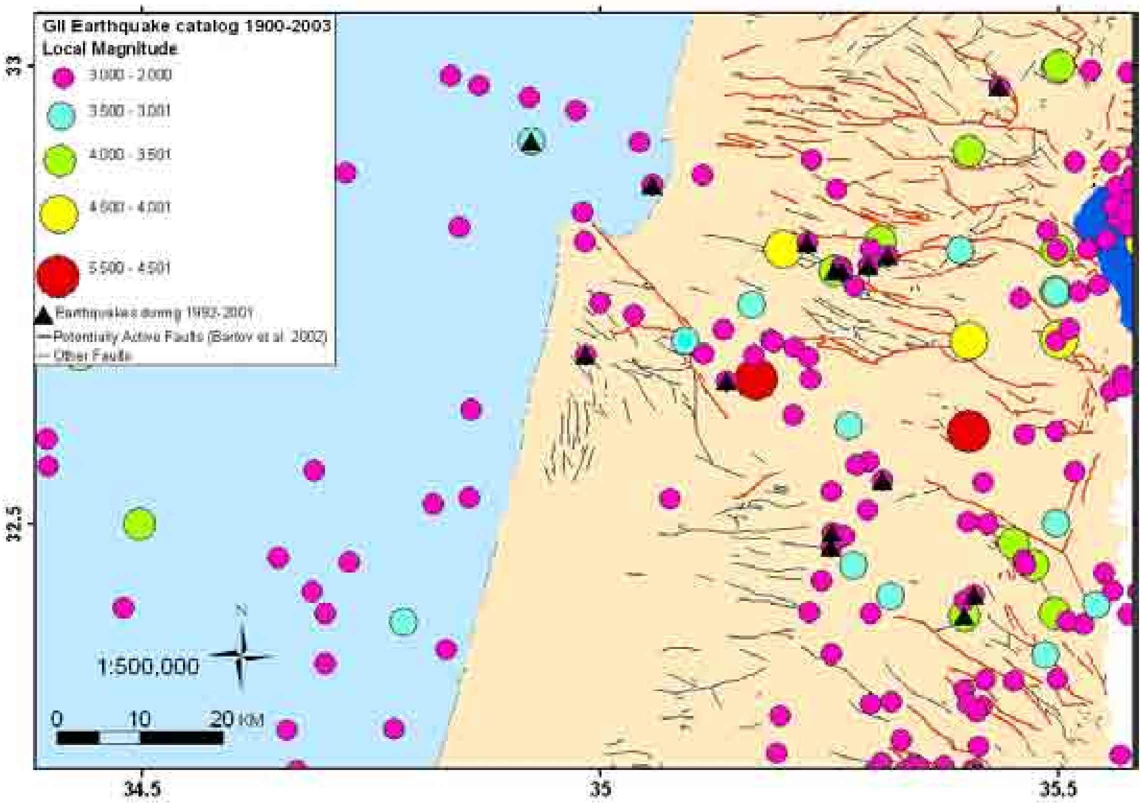

Fig 2. Earthquakes between the years 1900 - 2003 (GII catalog). Black triangles mark earthquakes during 1992-2001.

3. Permanent Scattering Interferometric Synthetic Aperture Radar (PSInSAR)

3.1 Method

Until recently, only conventional InSAR methods were used for high-resolution deformation studies in Israel (e.g., Baer et al., 1999). We present here the first use in Israel of the Permanent Scattering (PS) InSAR technique.

Interferometric techniques involve phase comparison of synthetic aperture radar (SAR) images, gathered at different times with slightly different looking angles. They carry the potential to detect millimetric target displacements along the satellite's Line-Of-Sight (LOS) direction. Apart from cycle ambiguity problems, limitations are due to temporal and geometrical decorrelation, and to atmospheric artifacts.

Temporal decorrelation makes interferometric measurements unfeasible where the electromagnetic profiles and/or the positions of the scatterers change with time within the resolution cell. In addition, atmospheric heterogeneity creates an atmospheric phase screen (APS) superimposed on each SAR image that can seriously compromise accurate deformation monitoring. Indeed, even considering areas slightly affected by decorrelation, it may reveal extremely difficult to discriminate the signal of interest and the atmospheric signature, at least using individual interferograms (for more details on conventional InSAR, see Baer et al., 1999 and references therein).

The PS approach is based on a few basic observations (summarized from the TRE web site: http://213.215.195.35/tresite_eng/tecnicaps/subtecnicaps/interferometria/index.htm) Atmospheric artifacts show a strong spatial correlation within every single SAR acquisition, but they are uncorrelated in time. Conversely, target motion is usually strongly correlated in time and can exhibit different degrees of spatial correlation depending on the phenomenon at hand (e.g. subsidence due to water pumping, fault displacements, localized sliding areas, collapsing buildings, etc.). Atmospheric effects can then be estimated and removed by combining data from long time series of SAR images, such as those available in the ESA-ERS archive, gathering data since late 1991. In order to exploit all the available images, and then improve the accuracy of the estimation, only scatterers slightly affected by both temporal and geometrical decorrelation are selected.

Possible stable and point-targets, hereafter called **Permanent Scatterers (PS)**, are detected on the basis of the stability of their amplitude returns. This allows pixel-by-pixel selection with no spatial averaging. Due to high spatial correlation of the PS, even a sparse grid of measurements may allow proper sampling of the atmospheric components, provided that the PS density is larger than 3-4 PS/km^2. Of course, a sufficient number of images should be available (usually more than 30), in order to properly identify PS and separate the different phase contributions. Relative target LOS velocity can be then estimated with unprecedented accuracy (often better than 0.1 mm/yr, due to the long time span). The final results of this multi-interferogram approach is a table of the PS identified in the image and their coordinates: latitude, longitude and their average LOS velocity. For some of points an additional table is given, that also includes the estimated motion component of each PS as a function of time. Common to all differential interferometry applications, the results are computed with respect to a ground control point (GCP) of known elevation and motion.

3.2 Results

3.2.1 Conventional InSAR

Conventional InSAR results of both ascending (Fig. 3) and descending (Fig. 4) tracks show significant loss of coherence, particularly in the agricultural areas of Yizre'el Valley, Zevulun plane and the Mediterranean coast west of Mt. Carmel. Short-wavelength atmospheric artifacts are also prominent (Figs. 3, 4). The results of this method have not yet been researched and only shows future research method.

3.2.2 PSInSAR

PSInSAR analysis overcomes some of these problems. Two major deformation features are outlined by the average annual velocity map (Fig. 5): (1) subsidence in the area of the Zevulun plane, particularly near the outlet of the Kishon River; (2) uplift in the areas of Tiv’on Hills and on the eastern part of Menashe Hills. In the northern part of the Mt. Carmel, where the city of Haifa is located, there is no distinct deformation pattern, however, in general, uplift may be inferred in the center of this area, surrounded by subsiding slopes. The major part of Mt. Carmel is a national forest with a relatively small number of permanent scatterers.

3.2.2.1 The Lev-Hamifratz Area

In the Lev-Hamifratz shopping center, where significant subsidence is observed, a good correlation is found among 10 different PS points (Fig. 6). Lev-Hamifratz was opened to the public in 1991, just before the acquisition of ERS data. Subsidence in this area is at constant rates of about 7 mm/y during the entire period of 9 years. Such linear rate is not likely to be a result of compaction due to ground settlement following a new construction, however it might be connected to subsidence of thick layers of black clays shown in drilling logs in this area.
In a short visit to the shopping center, large cracks were observed at the entrance of the parking lot (Fig. 7) as well as in the building itself. Significant subsidence was observed along the pavement (Fig 8) and the road leading to the main entrance. Additional work is required to better understand the subsidence observed in that area.

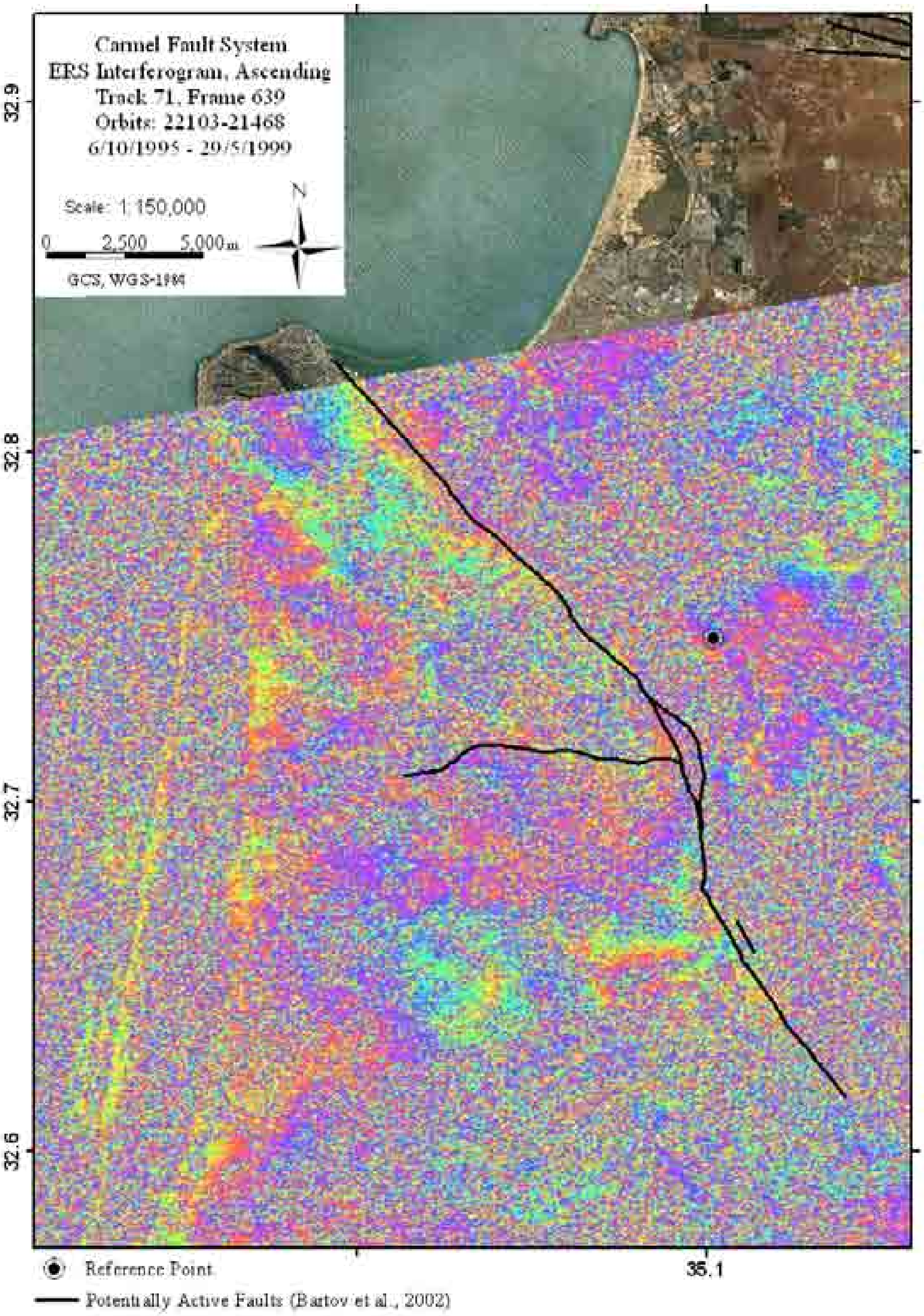

Fig 3. ERS SAR wrapped interferogram 6/10/1995 – 29/5/1999 (ascending track).

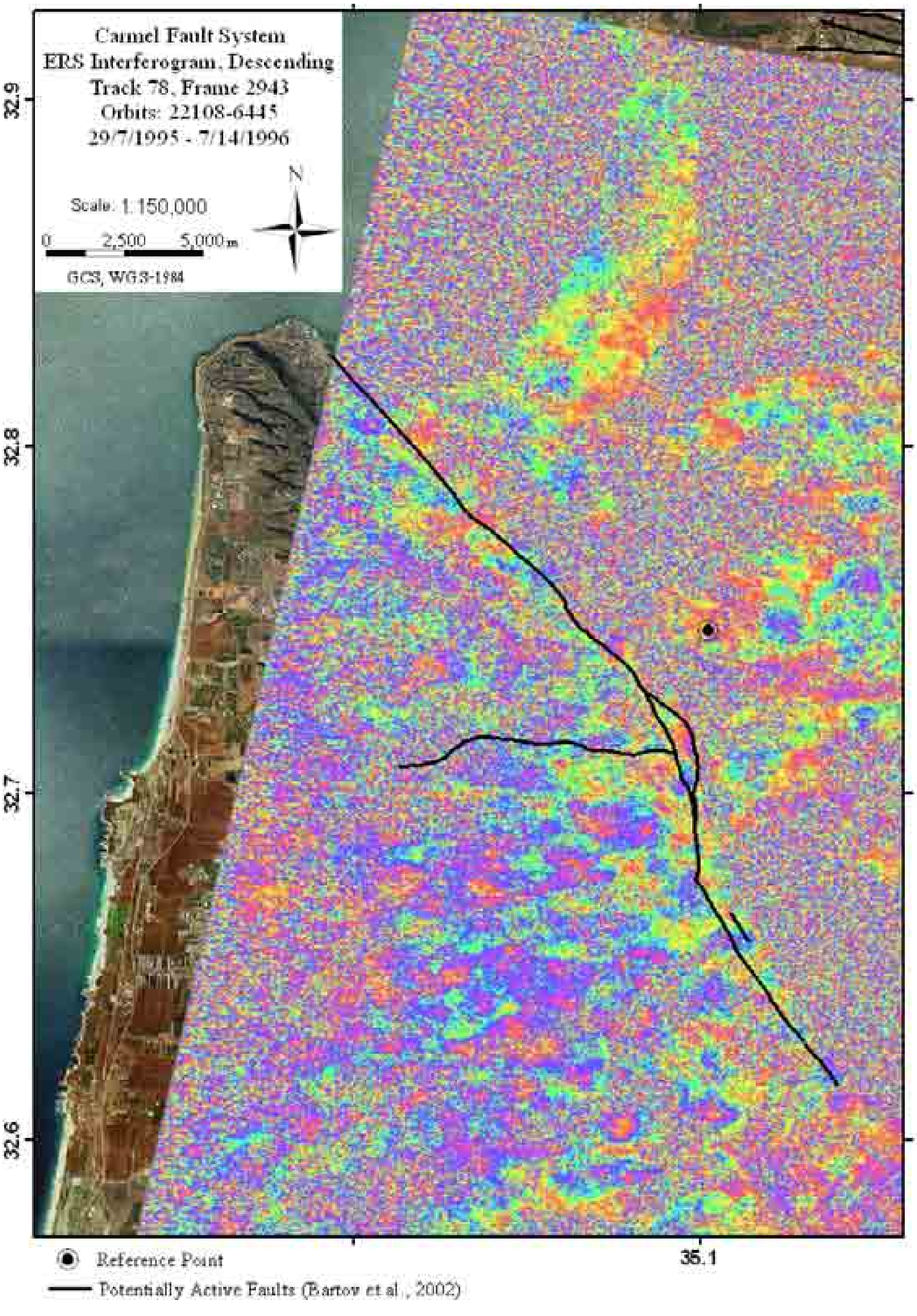

Fig 4. ERS SAR wrapped interferogram, 29/7/1995 – 7/14/1996 (descending track).

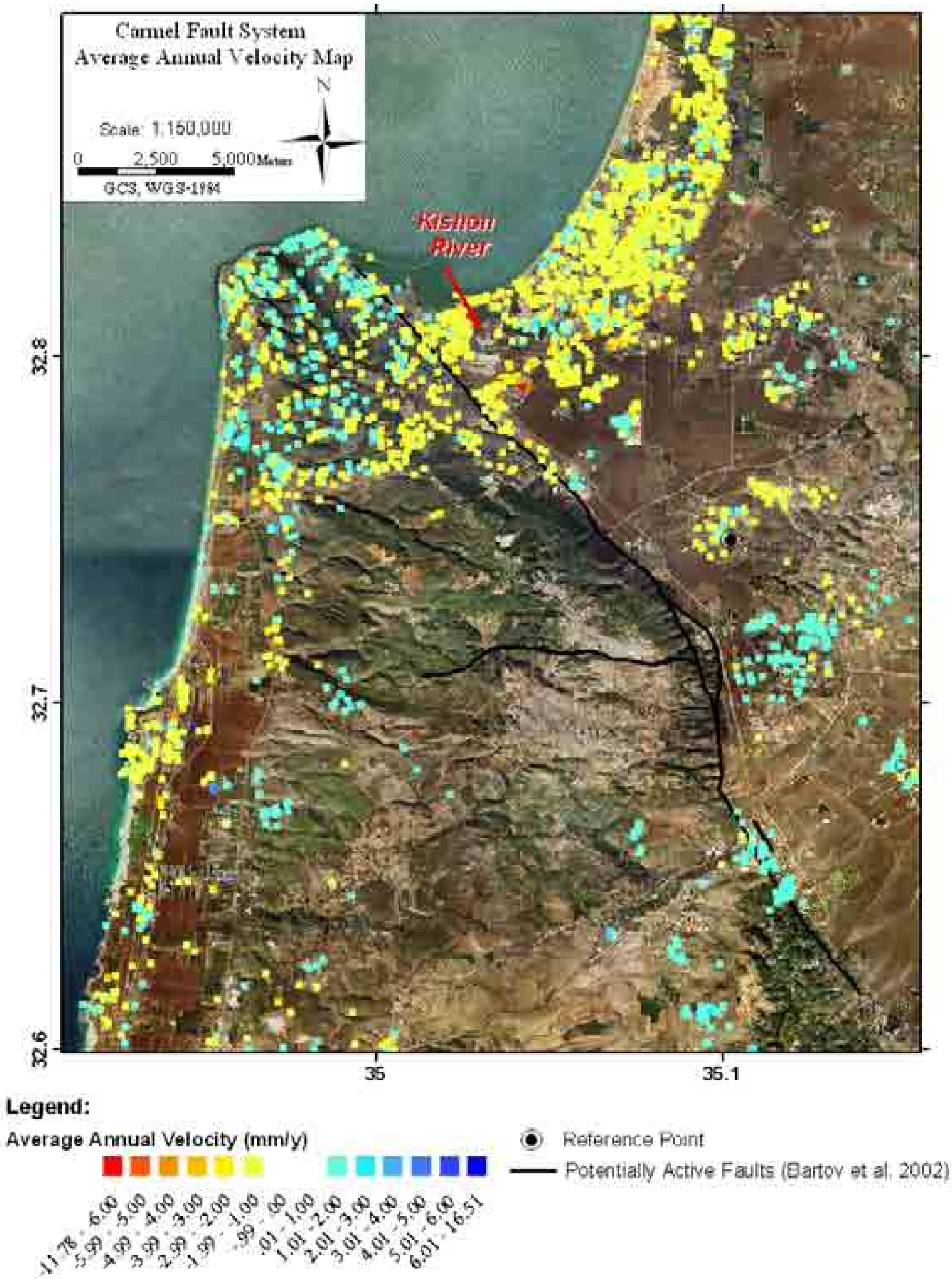

Fig 5. PSInSAR average annual velocity map. Values between -1 and 1 mm/y have been omitted from the plot for a better view.

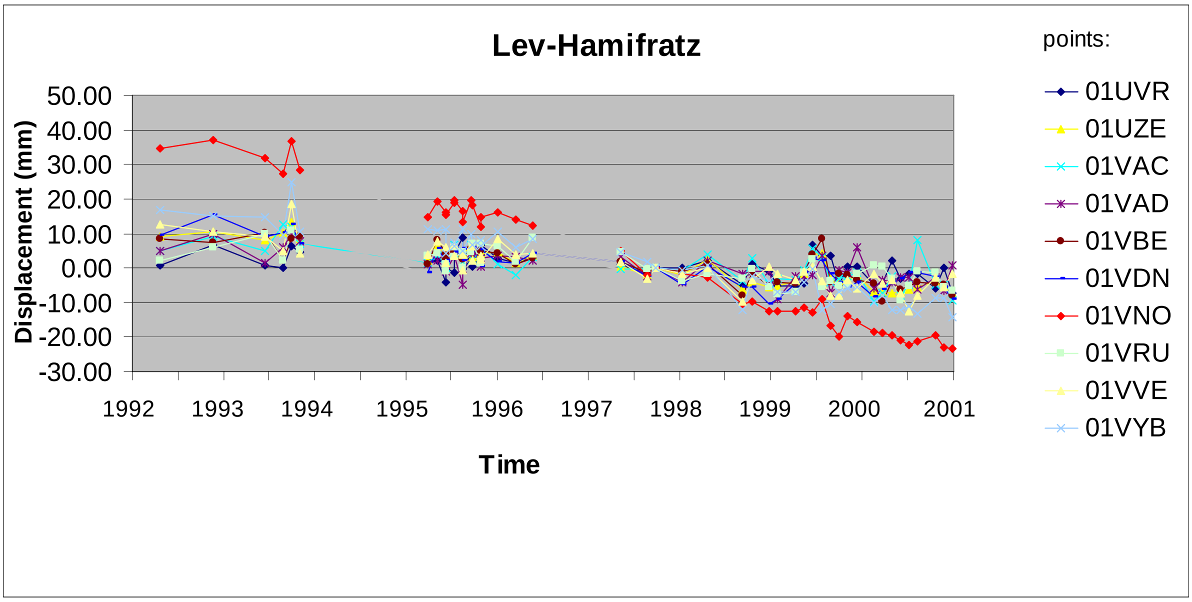

Fig 6. Lev-Hamifratz area, time-series of 10 subsiding points (see Fig. 11 for location).

3.2.2.2 The Rupin Bridge

An interesting location where subsidence has been observed is the Rupin Bridge (Fig. 9). The Bridge was built in 1990 and was repaired in 1991-1992 after cracks appeared due to foundation subsidence. The time series of PS points situated exactly on top of the bridge (Fig. 10) show very good correlation to each other until the beginning of 2000, when rapid subsidence is shown on one point for a time of a year until the beginning of 2001. Being a major connecting road for several neighborhoods in Haifa it is suggested for further investigation.

Fig 7. The northern wall of the eastern entrance
To Lev-Hamifratz shopping center parking.

Fig 8. Pavement on the western entrance to
Lev-Hamifratz shopping center parking.

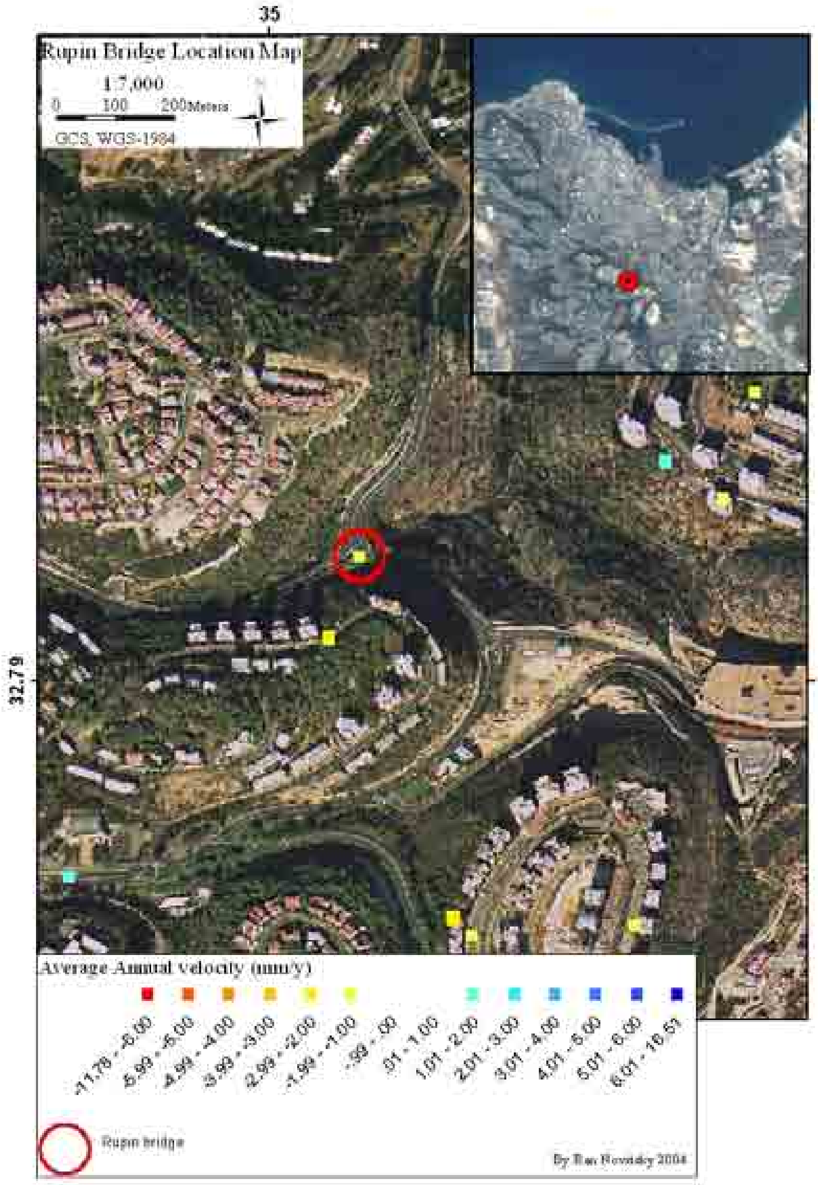

Fig 9. Rupin Bridge location map.

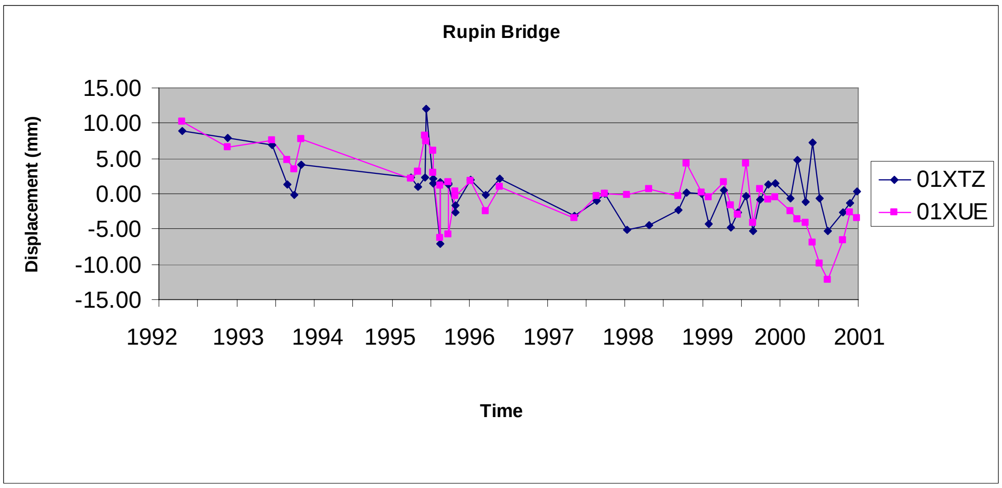

Fig 10. Rupin Bridge time-series of 2 points.

4. Discussion

4.1 Integration with other Information Sources

Using ArcGIS system, the PSInSAR data was integrated with earthquake catalogues, conventional InSAR data, water-level measurements, geological and lithological maps, slope maps, and an elastic dislocation strike-slip fault model. In the following sections, an attempt is made to correlate the observed deformation with its possible sources.

4.1.1 Seismicity

No deformation can be directly correlated to seismic activity. The GII earthquake catalogue shows no significant seismicity during the years 1992-2001 (Fig. 2). Only 4 earthquakes, all below M_L=3.5 and deeper than 10 km, occurred in the vicinity of Haifa. It should be considered, however, that tectonic movement along the CFS might be aseismic (creeping), and under that mode could lead to some of the observed deformation (see below). The tectonic mechanism observed by the InSAR method might be correlated with earthquake focal solutions mechanism (work is underway).

4.1.2 Water-level changes

The area of Haifa Bay, particularly near the outlet of the Kishon River, shows significant subsidence. It consists of clays and sand and the groundwater table is close to the surface. The Zevulun Plane has been intensely drilled for water. We checked four water wells which are located as close as possible to the area that shows the highest subsidence rate (Fig. 11). Figure 12 shows a very good correlation among water level changes in all four wells. However, a comparison between one of these well logs (the most complete) and 5 adjacent PS time series points which are approximately at the same distance from the wells (Fig. 13) shows no correlation. The good correlation between the water well logs is in contrast with the poor correlation between the PS time series. We note that there is some correlation between the general trend (subsiding) of the water level and average deformation of the subjected points that needs further investigation.

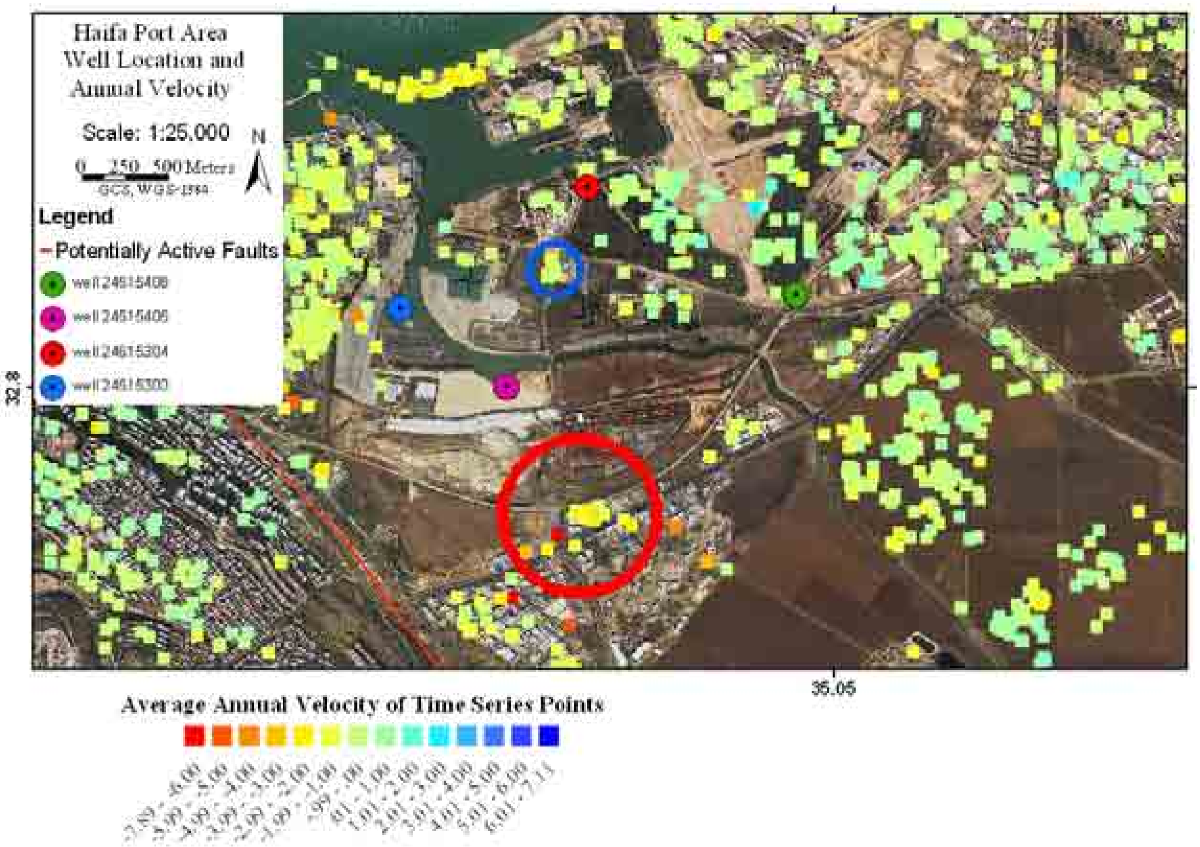

Fig 11. Haifa Port area, Wells and average annual velocity of time-series points. Blue circle surrounds the points used to correlate water-levels and deformation (Fig. 12). Red circle is Lev-Hamifratz area (see 3.2.2.1).

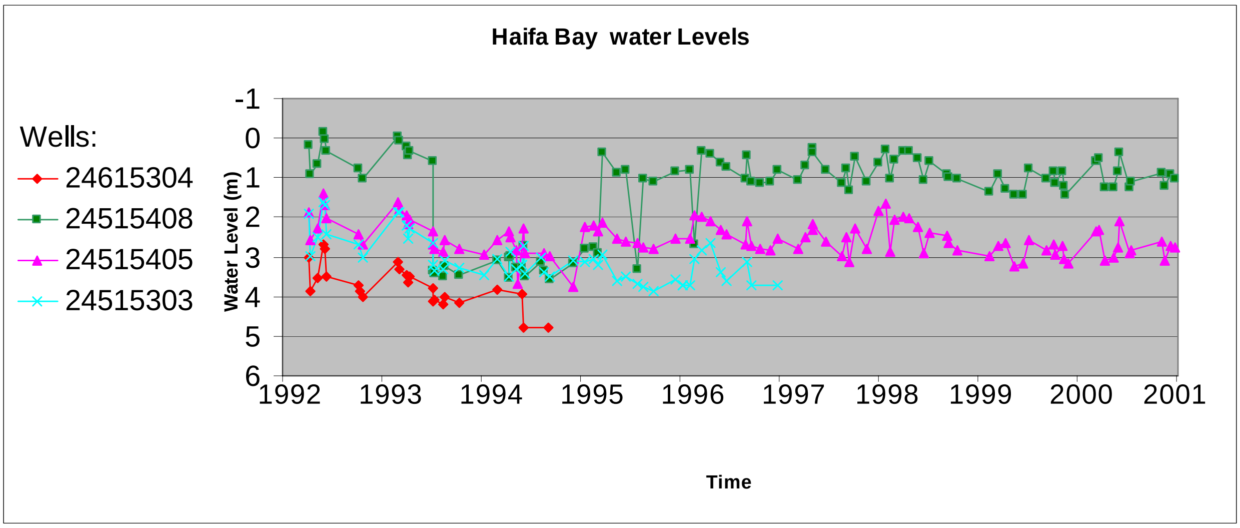

Fig 12. Water levels in 4 wells at the outlet of the Kishon River.

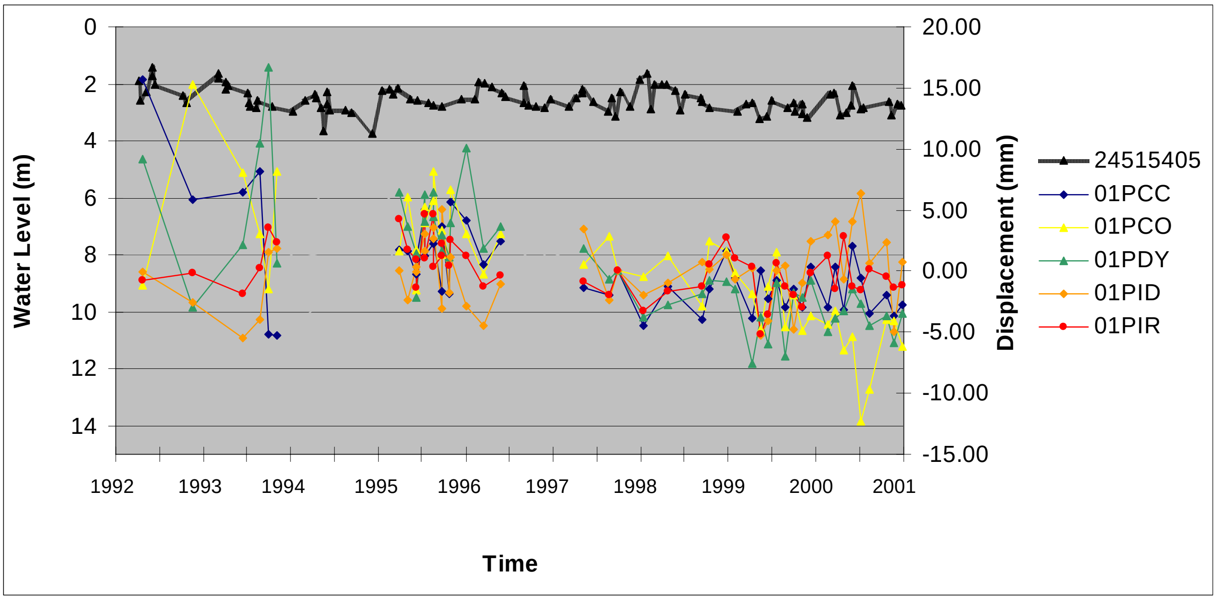

Fig 13. Water levels and time-series of points adjacent to the Haifa-Bay wells (Fig 12). Bold line marks the well water-level.

4.1.3 Landslides

Landslides may be a possible explanation to some of the observed movements mainly on the slopes of Mt. Carmel where soft rocks (chalk, clay, or marl) are present. An attempt to correlate subsiding points on Mt. Carmel with landslides and with a landslide sensitivity map was made. We used a DEM-derived slope map and a lithological map derived of 1:50,000 geological map to construct a landslide sensitivity map. A cross correlation between the subsiding points and the landslide sensitivity map (Fig. 14) shows that most of the subsiding points are not correlated with known or potential landslides. Moreover, no correlation between subsidence rate and degree of landslide sensitivity is apparent. Thus, the cause of the observed subsidence along the slopes is still unclear.

4.1.4 Tectonic Model

Tectonic models for the CFS may partly explain some of the observed deformation. As proposed by Achmon (1998 ; Fig 15) compression, push-up structures and uplift are expected along the NS-striking segment of the CFS and may explain the observed uplift in the western Menashe and Tivon Hills, and the subsidence at the Kishon Graben area. A more thorough analysis of the recent movements along the CFS and the resulting deformation in the adjacent blocks is currently underway.

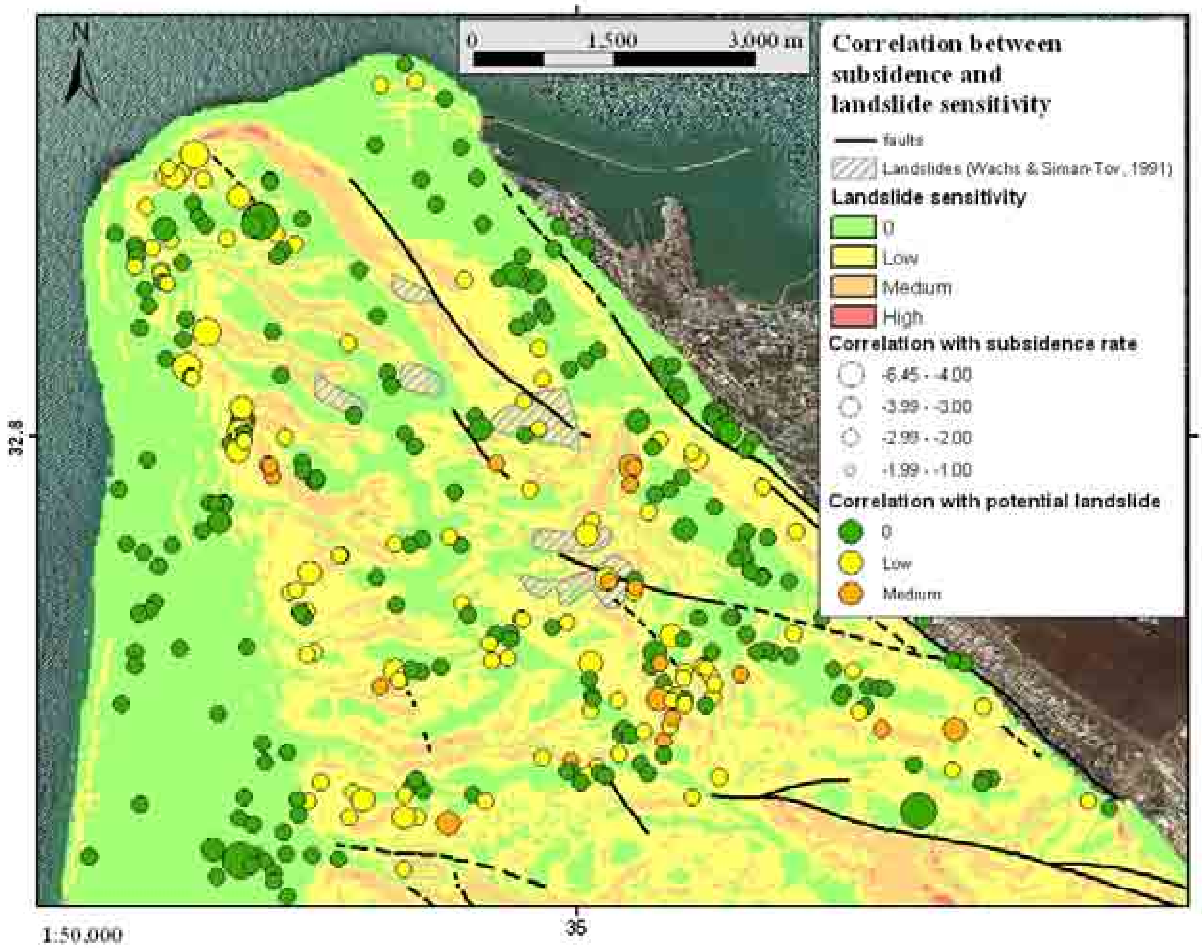

Fig 14. Landslide sensitivity map and correlation with subsiding points. Size of points marks the average annual velocity. Color of points marks the point's potential of being a landslide.

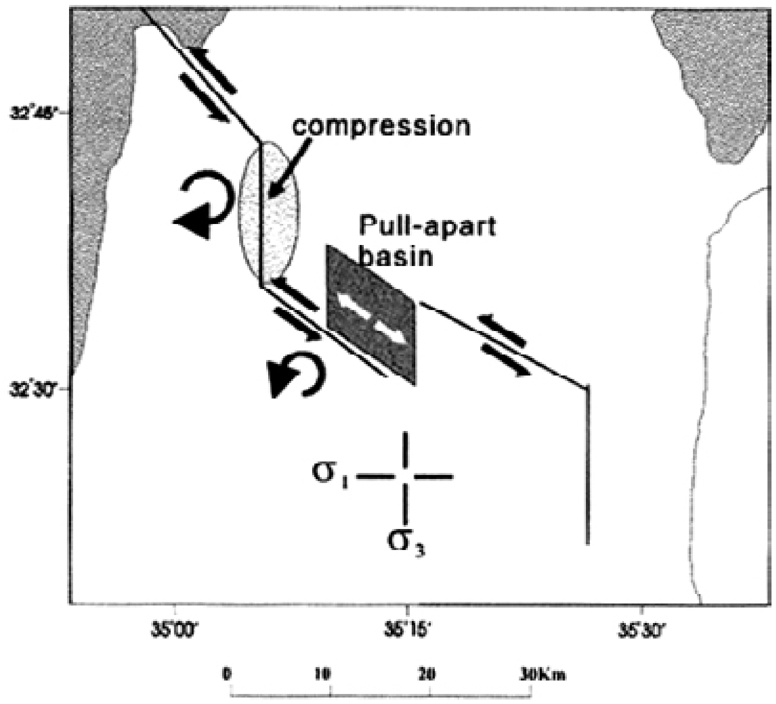

Fig 15. Strike-Slip Fault model (Achmon, 1998).

5. Summary and Conclusions

This preliminary report shows the advantages of the PSInSAR. It has the potential to overcome the atmospheric decorrelation, as well as producing precise point data. Nevertheless, this method gives results for mostly man-made structures. It does not measure most vegetated areas and is thus limited in its spatial coverage.

So far we observed no direct correlation with seismic activity, water-levels change or landslide potential. However, we managed to partly explain some of the results by observing deformed structures or by correlation with a tectonic model. More work is needed to figure out the mechanism of the various deformation features. Conventional InSAR processing of the area is underway, and may help to better understand the regional deformation and its mechanism, allowing an improved assessment of the seismic risk along the CFS and its vicinity.

6. REFERENCES

Achmon, M., 1986, The Border Fault of the Carmel Between Yokneam and Nesher, MS.c. Thesis, Hebrew University, Jerusalem

Achmon, M., 1998, Paleomagnetic and Geophysical Research of the Carmel Fault Zone, Ph.D. Thesis, Tel-Aviv University, Tel-Aviv.

Baer, G., Sandwell, D., Williams, S., and Bock, Y., 1999, Coseismic Deformation Associated with the November 1995, Mw=7.1 Nuweiba earthquake, Gulf of Elat (Aqaba), Detected by Synthetic Aperture Radar Interferometry, J. Geophys. Res., 104, 25221-25232.

Bartov, Y., Sneh, A., Fleischer, L., Arad, V. and Rosensaft, M., 2002, Map of Potentially Active Faults in Israel, Geological Survey of Israel, Rep. GSI/29/2002.

De-Sitter, L.U., 1962, Structural Devlopment of the Arabian Shield in Palestine. Geol. en. Mijnb., v. 45, p. 116-124.

Freund, R., 1965, A Model of Structural Development of Israel and Adjacent Areas Since the Upper Cretaceous Times, Geol. Mag., 102, 189-205.

Ginzburg, A., Ben-Avraham, Z., Makris, J., Hubral, P., and Rotstein, Y., 1994, Crustal structure of northern Israel: Mar. Petrol. Geol., v. 11, p. 501-506.

Gluck, D., 2001, The Landscape Evolution of the Southwestern Dead-Sea Basin and the Paleoseismic Record of the Southwestern Marginal Fault of the Dead-Sea Basin and of the Carmel Fault During the Late Pleistocene and the Holocene, MS.c. Thesis, Hebrew University, Jerusalem.

Heimann, A., Frydman, S., Wachs, D. and Talwani, P., 2001, Seismic hazard evaluation of Haifa and Eilat Bay areas, Geological Survey of Israel, Rep. GSI/40/2001

Hofstetter, A., van Eck, T.J., and Shapira, A., 1996, Seismic activity along fault branches of the Dead Sea-Jordan transform system: The Carmel-Tirza fault system: Tectonophyics, 267, 317-330.

Kafri, U. and Ecker, A., 1964, Neogene and Quaternary Subsurface Geology and Hydrogeology of the Zevulun Plain. Geol. Surv. Isr. Bull., 37, 45 pp.

Rotstein, Y., Bruner, I., and Kafri, U., 1993, High-resolution seismic imaging of the Carmel fault and its implications for the structure of Mt. Carmel: Isr. J. Earth Sci., 42, 55-69.

Rotstein, Y., Shaliv, G., and Rybakov, M., 2003, Active Tectonics of the Yizre'el Valley, Israel, Using High-Resolution Seismic Reflection Data: Tectonophysics, 382, 31-50.

Shamir et al., 2000, Preliminary seismic zonation in Israel, GII Rep. No 550/95/01.

Wachs, D. and Siman-Tov, O., 1991, Preliminary Assessment of Seismic risk in Haifa and Zevulun plain, Israel: Jerusalem, Geological Survey of Israel, Rep. GSI/31/1991.